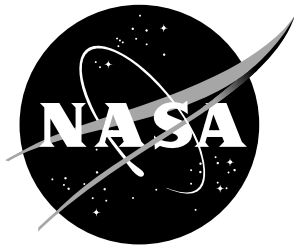


NASA/TM-20230000292



# High Intensity Modal Impedance Tube Development at NASA Langley

*Chelsea Solano, Michael G. Jones, Alexander N. Carr, Douglas M. Nark  
Langley Research Center, Hampton, Virginia*

---

February 2023

## NASA STI Program... in Profile

Since its founding, NASA has been dedicated to the advancement of aeronautics and space science. The NASA scientific and technical information (STI) program plays a key part in helping NASA maintain this important role.

The NASA STI Program operates under the auspices of the Agency Chief Information Officer. It collects, organizes, provides for archiving, and disseminates NASA's STI. The NASA STI Program provides access to the NASA Aeronautics and Space Database and its public interface, the NASA Technical Report Server, thus providing one of the largest collections of aeronautical and space science STI in the world. Results are published in both non-NASA channels and by NASA in the NASA STI Report Series, which includes the following report types:

- **TECHNICAL PUBLICATION.** Reports of completed research or a major significant phase of research that present the results of NASA programs and include extensive data or theoretical analysis. Includes compilations of significant scientific and technical data and information deemed to be of continuing reference value. NASA counterpart of peer-reviewed formal professional papers, but having less stringent limitations on manuscript length and extent of graphic presentations.
- **TECHNICAL MEMORANDUM.** Scientific and technical findings that are preliminary or of specialized interest, e.g., quick release reports, working papers, and bibliographies that contain minimal annotation. Does not contain extensive analysis.
- **CONTRACTOR REPORT.** Scientific and technical findings by NASA-sponsored contractors and grantees.

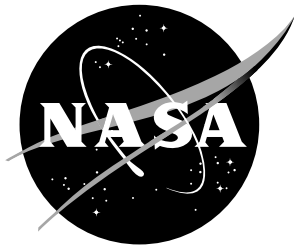
- **CONFERENCE PUBLICATION.** Collected papers from scientific and technical conferences, symposia, seminars, or other meetings sponsored or co-sponsored by NASA.
- **SPECIAL PUBLICATION.** Scientific, technical, or historical information from NASA programs, projects, and missions, often concerned with subjects having substantial public interest.
- **TECHNICAL TRANSLATION.** English-language translations of foreign scientific and technical material pertinent to NASA's mission.

Specialized services also include organizing and publishing research results, distributing specialized research announcements and feeds, providing information desk and personal search support, and enabling data exchange services.

For more information about the NASA STI Program, see the following:

- Access the NASA STI program home page at <http://www.sti.nasa.gov>
- E-mail your question to [help@sti.nasa.gov](mailto:help@sti.nasa.gov)
- Phone the NASA STI Information Desk at 757-864-9658
- Write to:  
NASA STI Information Desk  
Mail Stop 148  
NASA Langley Research Center  
Hampton, VA 23681-2199

NASA/TM-20230000292



# High Intensity Modal Impedance Tube Development at NASA Langley

*Chelsea Solano, Michael G. Jones, Alexander N. Carr, Douglas M. Nark  
Langley Research Center, Hampton, Virginia*

National Aeronautics and  
Space Administration

Langley Research Center  
Hampton, Virginia 23681-2199

---

February 2023

The use of trademarks or names of manufacturers in this report is for accurate reporting and does not constitute an official endorsement, either expressed or implied, of such products or manufacturers by the National Aeronautics and Space Administration.

Available from:

NASA STI Program / Mail Stop 148  
NASA Langley Research Center  
Hampton, VA 23681-2199  
Fax: 757-864-6500

# Abstract

A High Intensity Modal Impedance Tube (HIMIT) was developed for evaluation of acoustic liners in a normal incidence, high sound pressure level (SPL), and high frequency environment. Capabilities of the HIMIT are demonstrated here by testing three classes of acoustic liners: a narrow chamber liner, conventional single degree of freedom liners, and over-the-rotor liners. The experimental results are compared to results in NASA Langley’s Normal Incidence Tube (NIT) for validation. The Zwikker and Kosten Transmission Line (ZKTL) model is also compared to the HIMIT results for selected configurations to study applicability of the model at high SPLs and frequencies. The HIMIT and NIT impedance spectra compare favorably up to 3.0 kHz, which is the upper frequency limit of the NIT analysis. The ZKTL model was used at frequencies up to 6.0 kHz and showed good agreement with HIMIT results for the entire frequency range tested, indicating that the model may be used at high frequencies when the plane wave mode is dominant.

## 1 Introduction

Acoustic liners are typically installed in the nacelle walls of jet engines to reduce the amount of noise radiated to the communities surrounding airports. A common type of acoustic liner is a single degree of freedom (SDOF) liner, which is comprised of a wire mesh or perforate facesheet (FS), followed by a honeycomb core, and terminated by a rigid backing plate. The amount of noise reduction (attenuation) depends on an intrinsic parameter, acoustic impedance, that is related to the geometry of the individual components of these SDOF liners [1]. As such, the impedance is an important parameter for designing acoustic liners.

Experimental characterization of impedance is commonly performed in a normal incidence tube (NIT) as a first step for verifying liner designs, since the test is quick and easy [2]. However, techniques commonly used to deduce the liner impedance based on the two-microphone method (TMM) [3] are limited to test conditions where the acoustic field consists solely of plane waves. This can be an issue at high frequencies where higher-order modes (HOM) are cut on. The cut on frequency of the  $[m,n]$  mode in a rectangular duct is given by [4]

$$f = \frac{c}{2} \sqrt{\left(\frac{m}{a}\right)^2 + \left(\frac{n}{b}\right)^2}, \quad (1)$$

where  $c$  is the speed of sound,  $m$  is the vertical mode order,  $n$  is the horizontal mode order, and  $a, b$  are the side lengths of the duct. Therefore, in a  $2.0'' \times 2.0''$  square duct, the first higher-order modes cut on at approximately 3.4 kHz at ambient conditions. The two-microphone method cannot be used above this frequency.

The frequency range of liner characterization can be expanded by incorporating higher order mode propagation into the data acquisition and analysis methods. This approach has been demonstrated previously in normal incidence, higher-order mode test rigs [5–8]. The general rig design consists of a no-flow waveguide with a number of microphones flush-mounted along the inner walls with a speaker and

test specimen mounted on either end. The number of microphones is dependent on the number of modes to be measured. For example, in the case of four modes propagating toward the liner and four propagating away from the liner, eight modes would be cut on necessitating a minimum of eight microphones. Abom [6] and Schultz et al. [7] used eight to ten microphones to accurately measure the first eight modes and analyzed the data with a direct modal decomposition method (MDM). A comparison of the impedance eduction in the plane wave regime saw alignment between the modal decomposition method and the TMM to within 95% confidence of the TMM results [7].

NASA Langley’s liner physics team recently developed a test rig that supports higher order mode propagation and measurement called the High Intensity Modal Impedance Tube (HIMIT) [5]. The 2.0”×2.0” square cross-section tube contains eight microphones, enabling testing at frequencies up to 6.0 kHz to evaluate modal content. A unique feature of this test rig is its ability to generate high sound pressure levels (SPLs). By introducing a Hartmann generator, SPLs up to 170 dB may be achieved. Jones et al. [5] first demonstrated the HIMIT by testing two well-known samples: a narrow chamber liner and an SDOF liner. The two liners were tested at 120 dB up to 6.0 kHz and 155 dB up to 3.0 kHz. The results up to 3.0 kHz aligned well with the NIT results of the same samples, validating both the impedance eduction technique and the experimental setup.

The work described here follows the study of Jones et al. [5] to further evaluate the HIMIT test capabilities. This includes testing five different liners – one narrow chamber, two SDOF, and two over-the-rotor – and testing at a finer frequency resolution and an additional SPL. The experimental results are compared to impedances educed with the data measured in the NIT and impedances predicted with analytical models to validate the results up to 6 kHz. The results presented here will be used for a qualitative comparison; a more detailed quantitative analysis will be part of future work. The paper is organized as follows. Section 2 describes the experimental setup and the test articles that are evaluated here. Section 3 presents experimental results in the HIMIT. Finally, Section 4 provides concluding remarks and future work the NASA Langley Liner Physics Team wishes to accomplish with the HIMIT.

## 2 Experimental Setup

### 2.1 Setup

A schematic of the HIMIT is shown in Figure 1. The setup is an impedance tube with two speakers on one end and a sample on the other. The tube has a 2.0”×2.0” square cross section with a distance of 14.0” between the speakers and sample. The higher-order mode cut on frequencies, calculated using Equation 1, are shown in Table 1. Between the two ends are nine flush-mounted microphones where eight 0.125” microphones are mounted in rotating plugs and one 0.25” microphone is mounted in the tube 0.25” away from the sample. The standalone microphone is referred to as the reference microphone, or “Ref Mic” in Figure 1, and is used to set the SPL at the sample. There are four rotating plugs, each with two microphones

spaced 1.25" (d) apart. Two plugs are mounted in the side wall while the other two are mounted in the top wall. The plugs can rotate in the tube to allow different measurement points along the duct to accurately capture higher order modes. The centers of plugs 1 and 3 are the same distance from the sample at a distance of 3.125" (r) from the sample while plugs 2 and 4 are 9.250" (r+s) away from the sample. The configuration of the plugs tested here is shown in Figure 1, with plugs 1 and 4 rotated 30° relative to the horizontal and plugs 2 and 3 rotated 60°.

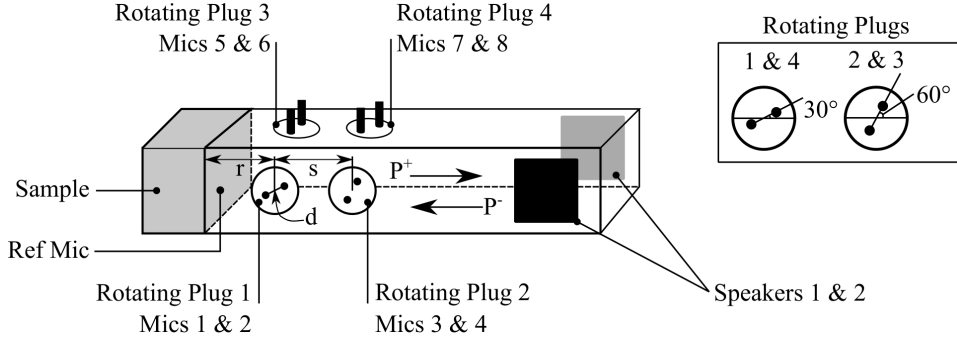


Figure 1: Schematic of HIMIT and annotation of rotating plug orientation.

Table 1: Cut on frequencies of HIMIT in standard sea-level dry air conditions based on Equation 1.

$[m, n]$	0	1
0	0.00 kHz	3.38 kHz
1	3.38 kHz	4.77 kHz

For the tests described here, the speakers generate tones in 0.2 kHz increments to produce an SPL at the reference microphone of 120 dB, 140 dB, or 150 dB, to within  $\pm 0.5$  dB. At 120 dB and 140 dB, the tested frequency range extends from 0.4 – 6.0 kHz, while at 150 dB SPL the tested frequency range is 0.4 – 3.0 kHz. Future studies will include data acquired with both high SPL ( $> 140$  dB) and high frequencies ( $> 3.0$  kHz). The microphone responses are sampled at 25.6 kHz and analyzed using a discrete Fourier transform with a frequency resolution of 6.25 Hz.

The plug microphones are calibrated using an in situ method described in Jones et al. [5] and briefly described here. The reference microphone is first calibrated using an external calibrator. A calibration test sample, named CSQ3 and to be described in Section 2.3, is mounted in the sample holder and the speakers are used to generate a 1 kHz tone. The SPL is set to 120 dB at the reference microphone; the phase of the reference microphone’s response is defined as 0 degrees. Acoustic pressures are measured with all rotating-plug microphones, with the plugs successively set to 0 and 180 degrees relative to the horizontal axis (following the switching two-microphone method). The acoustic pressures measured with the two microphones in plug 1 are used with the TMM [3] to determine the impedance at this frequency. With this information, the standing wave pattern in the duct is estimated. At this point, the pressure at each microphone is backed out from the standing wave

pattern and compared to the measurements for all eight measurement microphones to determine the sensitivity of the microphones.

## 2.2 Data Analysis

For general liner testing, a mode decomposition method (MDM), described in Jones et al. [5], is used to educe the acoustic impedance of the test liner mounted in the HIMIT. This method uses all eight measurement microphones to enable the sound field in the waveguide to be decomposed into modes, as long as no more than eight modes (four propagating toward the liner and four propagating away from the liner) are cut on. The normalized specific acoustic impedance can be expressed by

$$\zeta_{nm,nm} = \left( \frac{k}{k_x} \right) \frac{1 + R_{nm,nm}}{1 - R_{nm,nm}}, \quad (2)$$

where  $k$  is the free space wavenumber,  $k_x$  is the axial wavenumber, the reflection factor for the  $nm$  mode is  $R_{nm,nm} = A_{nm}^+ / A_{nm}^-$ , and  $A_{nm}^\pm$  are the reflected and incident mode amplitudes. The mode amplitudes can be used to calculate the pressure in the duct

$$p(x, y, z, t) = \sum_{n=0}^{\infty} \sum_{m=0}^{\infty} \left[ A_{nm}^+ e^{-ik_x x} + A_{nm}^- e^{ik_x x} \right] \cos\left(\frac{m\pi y}{H}\right) \cos\left(\frac{n\pi z}{W}\right) e^{i\omega t}. \quad (3)$$

This can be used to calculate the power in each mode

$$P_{nm}^+ = \frac{\epsilon_{nm}}{2} \frac{k_x}{\rho c k} \Re [A_{nm}^+ A_{nm}^{+*}], \quad (4)$$

where

$$\epsilon_{nm} = \begin{cases} WH, & \text{if } n = m = 0 \\ 0.5WH, & \text{if } n \neq 0 \text{ and } m = 0, \text{ or } n = 0 \text{ and } m \neq 0 \\ 0.25WH, & \text{if } n \neq 0 \text{ and } m \neq 0. \end{cases} \quad (5)$$

Both the normalized specific acoustic impedance and mode power will be evaluated in the results section.

## 2.3 Samples

The goal of this series of tests is to evaluate a range of liners, from simple to complex. Five samples are tested with descriptions and dimensions as listed in Table 2. The simplest sample in Table 2 is the test article named CSQ3, consisting of a narrow-chambered liner with an array of  $19 \times 19$  square cross section tubes, each with a cross section of  $0.05'' \times 0.05''$  and a chamber depth of  $3.0''$  (Fig. 2a). The liner is linear and has a predictable impedance with its large depth to chamber width ratio. This simple liner is not only used to evaluate the HIMIT but also used to calibrate the microphones (as described in the previous section, Section 2.1). The next liner sample, C15R27, is an SDOF liner consisting of a mesh over honeycomb (Fig. 2b). Complexity is added by removing the mesh top sheet and replacing it

with a perforate FS (shown in Fig. 2c), resulting in the liner sample GE01, which is frequently tested at the Liner Technology Facility (LTF). Next, two over-the-rotor (OTR) liners [9] are studied. The A015 OTR liner is an SDOF liner filled with metal foam and with grooves placed above the FS (see Fig. 2d). Finally, the A024 OTR liner is an expanded chamber design, see Fig. 2e. Rather than having cavity walls that are perpendicular from the FS to the backing plate, the walls narrow inwards and expand outwards to decrease and increase the cavity cross section, respectively. Although not pictured, grooves are also placed on top of the FS with dimensions as shown in Table 2. All liner samples are mounted onto the HIMIT as shown in Figure 1.

Table 2: Dimensions of the liners tested here. All dimensions are in inches unless otherwise noted.

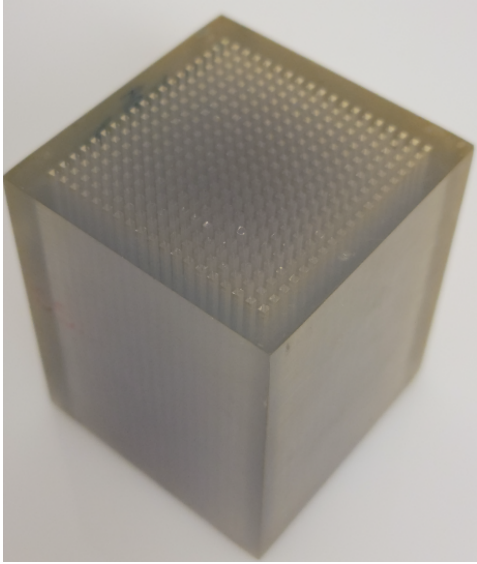
Name	Facesheet			Cavity		Grooves		
	Diameter	Thickness	POA	Width	Depth	Width	Rib	Depth
CSQ3	—	—	—	0.050	3.000	—	—	—
C15R27	—	—	—	0.375	1.500	—	—	—
GE01	0.039	0.025	8.7%	0.375	1.500	—	—	—
A015	0.035	0.060	10.0%	1.000	0.500	0.250	0.125	0.500
A024	0.035	0.060	10.0%	—	—	0.250	0.125	0.500

### 3 Results and Discussion

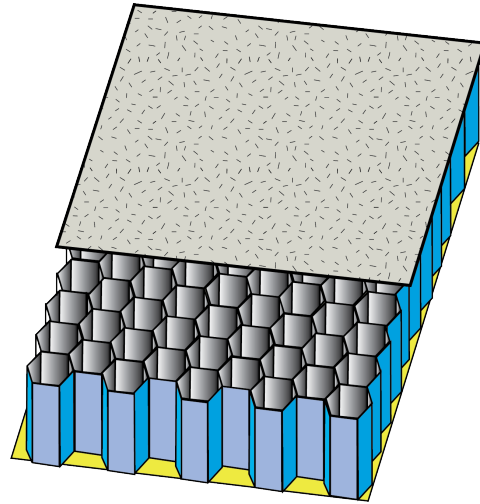
#### 3.1 Power Level

The total incident power level and incident power for each mode are plotted in Figures 3a – 3d for two liners: CSQ3 and A024. The incident power level curves for the other liners are similar to the results for CSQ3, shown in Figures 3a and 3b. For most of the frequency range, the plane wave is dominant. The only frequencies where the plane wave does not dominate are 3.8 kHz and 4.0 kHz. This happens to be true for all liners, including the calibration liner, SDOF liners, and OTR liners.

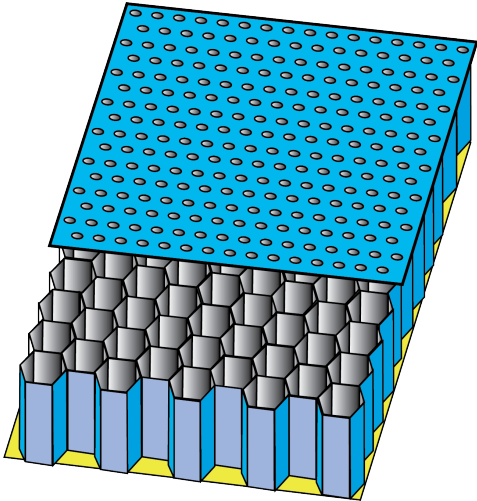
The prevalence of the (0,1) and (1,0) modes just below 4 kHz is likely a result of some intrinsic characteristic of the HIMIT causing the speakers to more effectively drive these HOM. Since the plane wave was not dominant between 3.8 – 4.0 kHz, difficulties were encountered when attempting to set the SPL at the reference microphone. Setting the SPL at the reference microphone is acceptable when plane waves are dominant since the acoustic pressure is nominally constant across the liner surface. However, when the frequency is sufficiently high to support higher-order modes, the acoustic pressure field may not be constant across the liner surface. For this condition, the current procedure for setting the incident level at the reference microphone is not a consistent approach. Different approaches to setting the incident level in the HIMIT will be investigated in the future to resolve this issue. However, for the current investigation we merely advise caution in interpreting results in the range 3.8 – 4.0 kHz.



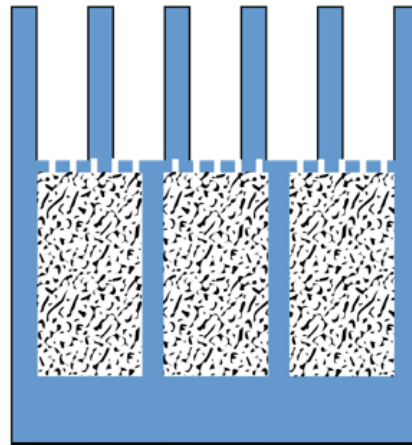
(a) CSQ3



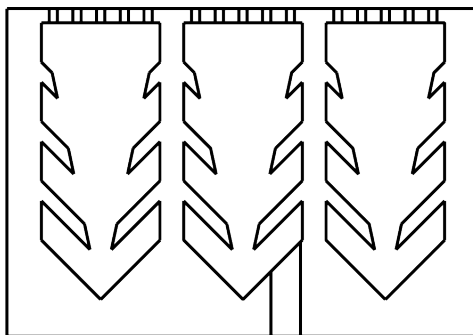
(b) C15R27



(c) GE01



(d) A015



(e) A024

Figure 2: Schematics of the samples tested in the HIMIT.

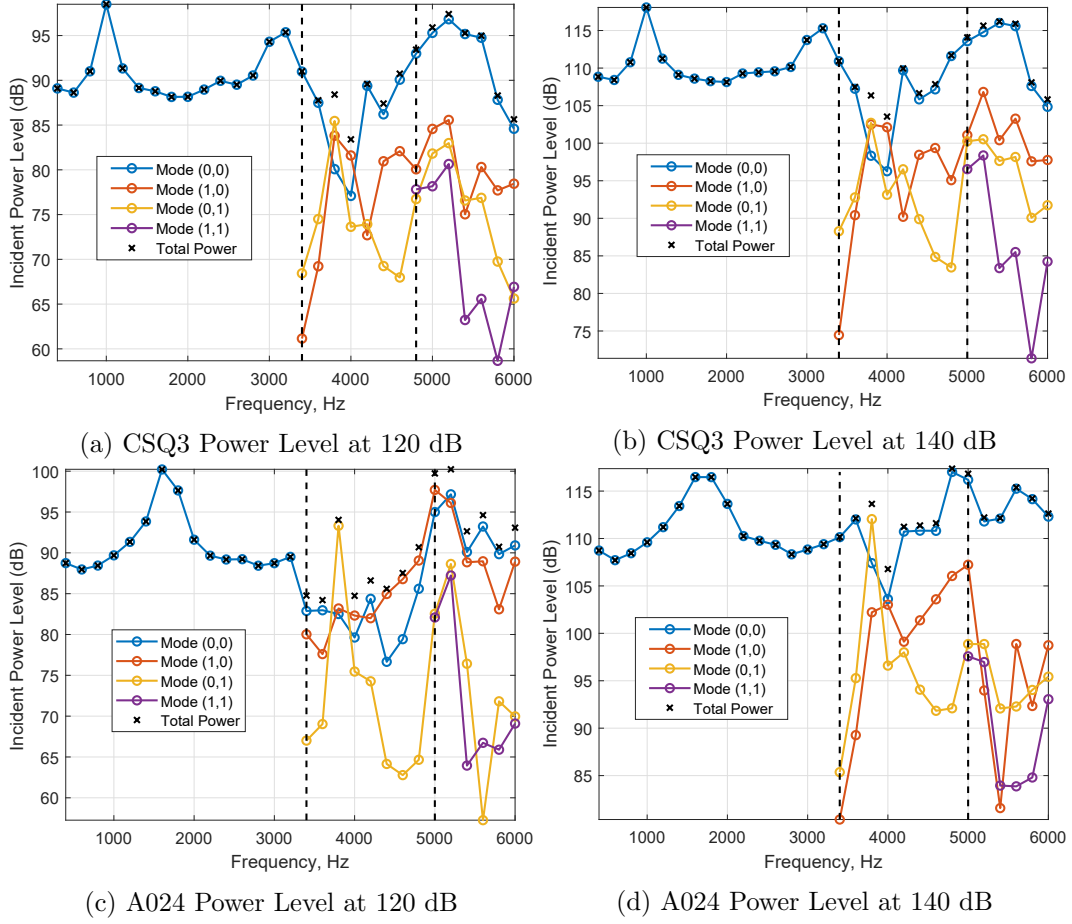


Figure 3: Power level plots of the samples CSQ3 and A024 at 120 dB and 140 dB.

An outlier of the power level data set is the results for liner A024 at 120 dB (see Fig. 3c). Rather than the plane wave mode dominating for the entire frequency range, mode (1,0) also has significant power. This could either be a liner dependent result or an anomaly since the higher power level is not seen for the 140 dB case (Fig. 3d). This will be explored further in future studies.

### 3.2 Impedance

The normalized specific acoustic impedance ( $\zeta = \theta + i\chi$ ), simply called impedance for the remainder of the paper, is plotted for each liner in Figures 4 - 8 for frequencies 0.4 - 6.0 kHz and SPLs 120 dB, 140 dB, and 150 dB. The 150 dB SPL case was only tested up to 3.0 kHz to focus on high levels without the complications of HOM. Educated impedances are indicated by the circles along the lines. Data at 3.8 kHz and 4.0 kHz are omitted since the plane wave mode does not dominate, as shown in Figure 3. Each figure contains at least two subplots with varying axis ranges, plotted with tight bounds unless otherwise noted. The liner impedance at the SPLs tested is plotted in subplot (a). Subplot (b) compares the 120 dB and 140 dB cases

to NIT results up to 3.0 kHz. Figures 4 - 6 have a third subplot (c), which compares the HIMIT results to an in-house ZKTL code [10] out to 6.0 kHz. Figures 7 - 8 do not have a subplot (c) since modeling the behavior of the A015 and A024 liners would require higher fidelity methods, beyond the scope of this work.

The impedance of the narrow chamber sample (CSQ3) is shown in Figure 4a. The impedance varies only slightly with SPLs across the entire frequency range. This was expected due to the linear nature of the liner, with a large depth relative to the cavity side length. The largest variation appears to be the 150 dB case near antiresonance at 2.0 kHz, where the results show a slight shift in the antiresonance peak. The HIMIT, NIT and predicted results align well in Figure 4b with an exception at antiresonance. This could indicate a mounting issue or that the MDM does not adequately resolve the impedance when there is minimal attenuation. The model and HIMIT results are plotted in Figure 4c for the entire frequency range tested and compares favorably. This indicates the model can be accurately used to predict the impedance even in the presence of higher-order modes, as least when plane waves are dominant.

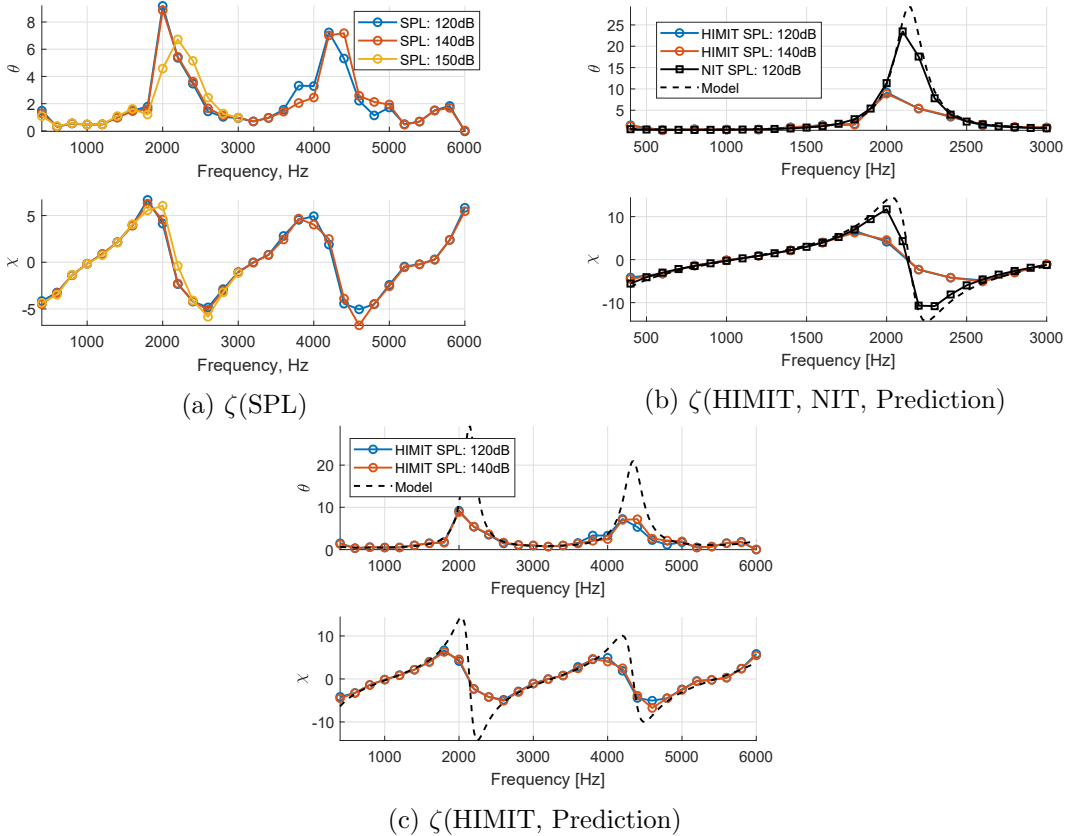


Figure 4: Impedance ( $\zeta$ ) of CSQ3 for varying SPLs tested in the HIMIT. The HIMIT results are also compared to NIT results and ZKTL predictions.

The impedance of C15R27 (mesh over honeycomb) is shown in Figure 5a. The impedance is invariant with SPL across the entire frequency range. This is expected

due to the linear nature of the wire mesh facesheet. NIT results are plotted in addition to the HIMIT results in Figure 5b; note the reduced y-axis range in the plot relative to 4b. The reactance shows good agreement while the HIMIT resistance values show increased variability. The variation between test rigs will be reevaluated with other samples to determine its importance. The predicted impedance of the liner is plotted in Figure 5b alongside the HIMIT and NIT results. The ZKTL model tracks very well with the reactance although it overshoots at antiresonance, likely due to the failure to include damping in this version of the model. The model compares favorably with the resistance, but the antiresonance peak is not predicted by the model. This was expected since the simplistic model used for this type of liner assumes a constant resistance equal to the manufacturer’s quoted DC flow resistance of 27 cgs rays and does not account for interaction between the resistance and reactance near antiresonance. Agreement is good at both SPL levels due to the linear nature of this liner.

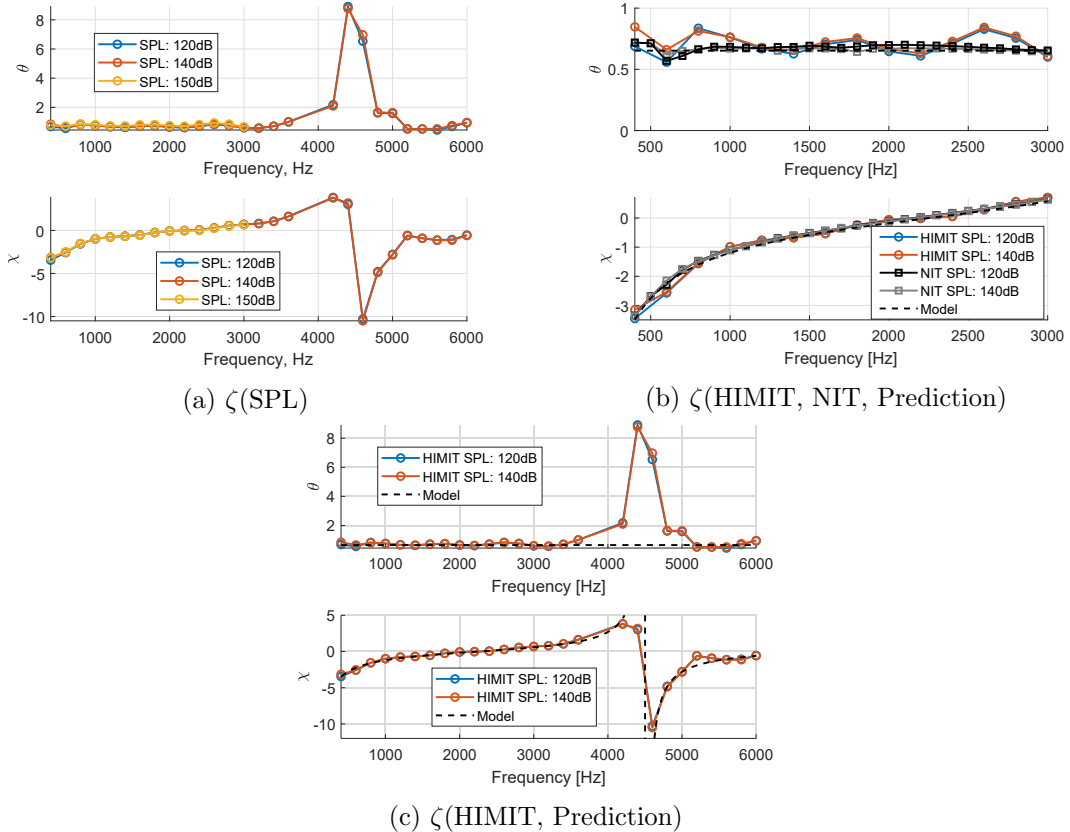


Figure 5: Impedance of C15R27 for varying SPLs tested in the HIMIT. The HIMIT results are also compared to NIT experimental results and ZKTL predictions.

The impedance of liner GE01 (an SDOF liner) is shown in Figure 6a. The impedance spectrum remains approximately the same for the different SPLs, with only a slight increase in resistance below 3.0 kHz with increasing SPL. The HIMIT results are compared to the ZKTL model and NIT results in Figure 6b, which shows

good agreement for the reactance where the lines are almost indistinguishable for the different cases shown. The educed resistance varies, between the two test rigs, but has approximately the same order of magnitude. The model and HIMIT results are plotted out to 6.0 kHz in Figure 6c. The model predicts the impedance well, including the antiresonance frequency. This suggests that the ZKTL model can be used while HOM are present but not necessarily while HOM are dominant. As observed with the C15R27 sample, it appears the resistance is higher overall in the HIMIT than in the NIT. Because the effect is seen across samples, it is likely due to the mounting procedure in the HIMIT or an issue with the MDM. Regarding mounting, the HIMIT sample is mounted to the end of the tube using a plate and four bolts. The plate is placed behind the liner and the bolts are used to press the plate and liner up to the side of the tube. The NIT sample on the other hand, is pressed up to the NIT using a plate and jack-screw mechanism, which provides a true uniform pressure distribution. It is possible that the bolting method does not provide uniform pressure across the liner. Both topics are the subject of an ongoing investigation.

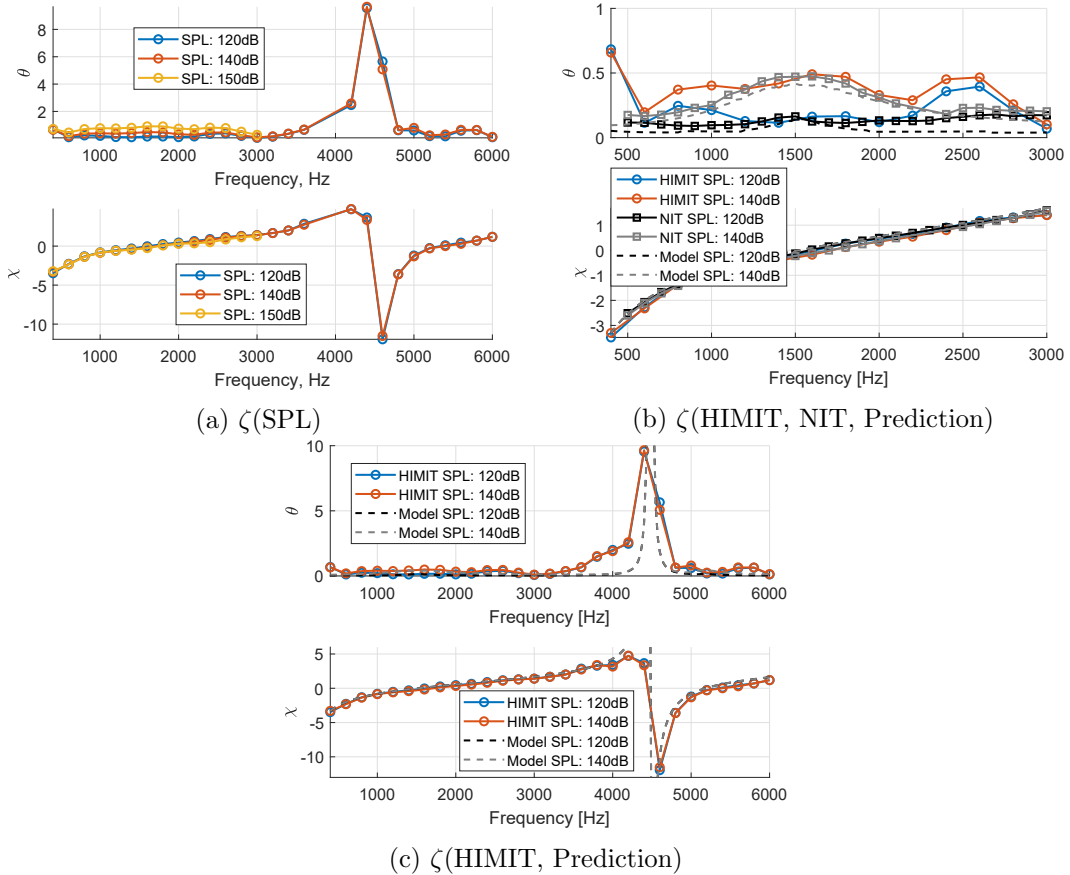


Figure 6: Impedance of GE01 for varying SPLs tested in the HIMIT. The HIMIT experimental results are also compared to NIT experimental results and ZKTL predictions.

The impedance for A015 (the SDOF liner filled with metal foam) is shown in Figure 7a. The reactance hovers near zero between 2.0 – 3.0 kHz except for frequencies near antiresonance, at which point the reactance crosses zero with a negative slope and a global maximum is reached in the resistance. Like the SDOF liners tested, the resistance for increasing SPL is slightly higher below antiresonance but is lower at the antiresonance peak. Figure 7b plots both the HIMIT and NIT impedances. The results between the two tests rigs align well below antiresonance. Near antiresonance, the resistance peak frequency is approximately the same between both test rigs and the reactance behavior appears to be approximately the same as well.

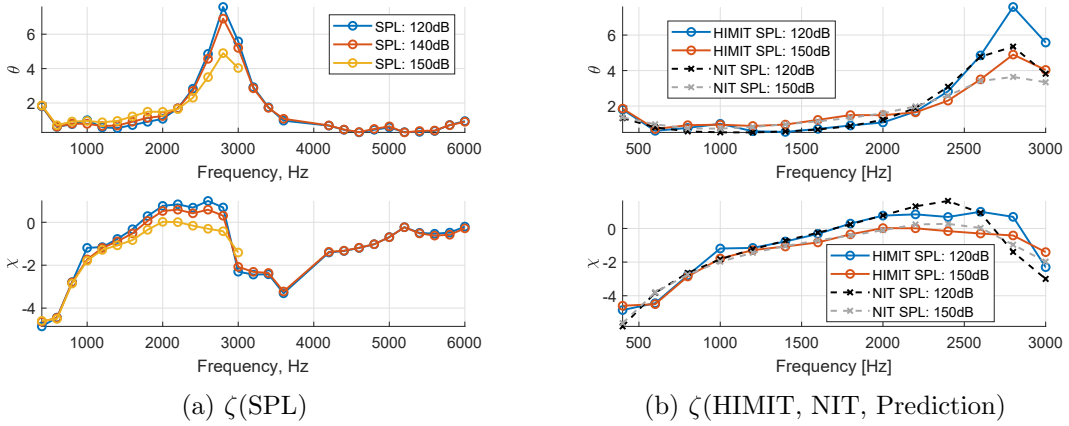


Figure 7: Impedance of A015 for varying SPLs tested in the HIMIT. The HIMIT experimental results are also compared to NIT experimental results and ZKTL predictions.

The impedance for A024 (the expansion chamber with a perforate FS) is shown in Figure 8a. The impedance has a similar trend to GE01 up to 4.0 kHz. Above that frequency the reactance appears to hover near zero with a weak antiresonance near 5.5 kHz. The resistance also has a similar trend to A015, with higher resistance values for increasing SPL below antiresonance. The HIMIT data is plotted with NIT results in Figure 8b. Away from antiresonance, the two measurements show excellent agreement, such that it is difficult to discern the different lines. This gives confidence in the HIMIT experimental setup and impedance eduction technique away from antiresonance.

Unlike all other liners evaluated here, for the A024 liner at 120 dB the plane wave was not dominant above 3.4 kHz. Instead, the plane wave (mode (0,0)) and mode (1,0) each dominated depending on the frequency. The impedance prediction for both dominant modes is shown in Figure 8c. Although either mode may have a higher power level for a given frequency, the impedance trend differs for the modes: mode (1,0) would indicate an additional antiresonance and essentially oscillates about the plane wave impedance. As mentioned, because both modes have approximately the same power level at higher frequencies, it is difficult to say which impedance curve is the obvious choice. Also, since there is no model to describe the liner impedance, we cannot be sure which mode is correct. However, based on the smooth nature of the impedances computed for the plane wave mode and agreement

between the impedances of the 120 dB and 140 dB plane wave mode in Figure 8a, it is likely that the plane wave mode is the correct choice. Liner impedance eduction under the influence of multiple dominant modes is a topic that needs further study.

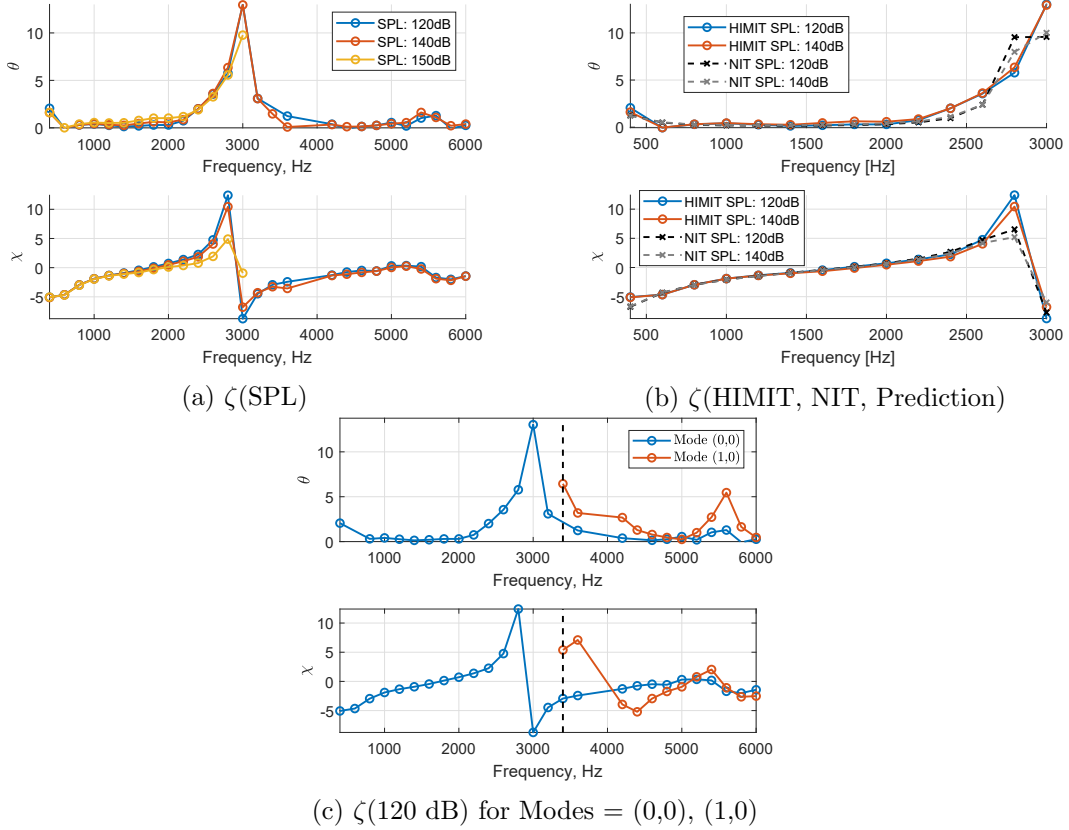


Figure 8: Impedance of A024 for varying SPLs tested in the HIMIT. The HIMIT results are also compared to NIT experimental results and ZKTL predictions.

## 4 Concluding Remarks

Five liners were evaluated using the newly built HIMIT test rig. Each liner was tested at three SPLs: 120 dB, 140 dB, and 150 dB, where 150 dB is considered a high SPL. The experiments were performed at 0.4 – 6.0 kHz for the two lower SPLs and 0.4 – 3.0 kHz for the highest SPL. High SPL, high frequency effects will be the subject of a future study. For four of the five liners, the plane wave was dominant for the tested frequency range except between 3.8 and 4.0 kHz. Between those frequencies, it is likely that the speaker arrangement and dimensions of the HIMIT resulted in the higher-order modes dominating. Therefore, only the plane wave impedance was presented for most cases.

The impedance trend between the different SPL levels remained approximately the same, consisting of an increase in the resistance with increasing SPL for liners

CSQ3, C15R27, and GE01, but a decrease in resistance for liners A015 and A024. The impedance results from the HIMIT compared favorably with results from the NIT for the SDOF liners but not as well for CSQ3 or the OTR liners. The ZKTL model was also compared to the HIMIT results for CSQ3, C15R27, and GE01; the other liners were too complex to be modeled by ZKTL and require higher fidelity modeling to accurately predict their impedance. The model accurately predicted the impedance for the entire frequency range of each liner modeled. This indicates that ZKTL can be used to model liners in the presence of higher order modes as long as the plane wave is dominant.

Continuing efforts on improving the test rig are under way. As observed in the results here, there could be slight mounting imperfections resulting in higher resistances than were measured in the NIT. Another potential issue could be failure of the modal decomposition method to adequately resolve the impedance when there is minimal attenuation. This is an issue with all impedance eduction methods and warrants further study. Additionally, the effect of simultaneously exposing liners to high frequencies ( $> 3$  kHz) and high SPLs ( $> 140$  dB) will be evaluated in future work.

Other concerns include how the SPL is set in the duct. Issues arise when setting the SPL at the sample surface when a higher-order mode is dominant over the plane-wave mode, as indicated in Section 3.1. SPL varies in the transverse direction of the duct for HOM. Thus, setting the SPL at the sample surface is not a consistent approach that should be used in the HIMIT when HOM are dominant, since the SPL will vary at the sample surface. Additional concerns arise from the possibility that the reference microphone is not representative of the SPL at the sample surface for high frequencies. This is because of the 0.25" standoff distance from the sample surface and the potentially significant axial changes in the standing wave pattern at those high frequencies. Future work will investigate alternative approaches to setting the level in the HIMIT that resolve these issues.

## References

1. R. E. Mottsinger and R. E. Kraft. *Aeroacoustics of Flight Vehicles: Theory and Practice, Volume 2: Noise Control*, chapter 14. Acoustical Society of America, New York, 2 edition, 1995.
2. M. G. Jones, W. R. Watson, D. M. Nark, B. M. Howerton, and M. C. Brown. A review of acoustic liner experimental characterization at NASA Langley. NASA/TP-20200003112, 2020.
3. ASTM E1050-98. Standard test method for impedance and absorption of acoustic materials using a tube two microphones and a digital frequency analysis system, 1998.
4. D. T. Blackstock. *Fundamentals of physical acoustics*, chapter 12. John Wiley & Sons Inc., 2000.

5. M. G. Jones, A. N. Carr, D. M. Nark, and L. E. Becker. Implementation of the NASA High Intensity Modal Impedance Tube. NASA/TM-20220017773, 2022.
6. M. Åbom. Modal decomposition in ducts based on transfer function measurements between microphone pairs. *Journal of Sound and Vibration*, 135(1):95–114, 1989.
7. T. Schultz, L. N. Cattafesta III, and M. Sheplak. Modal decomposition method for acoustic impedance testing in square ducts. *The Journal of the Acoustical Society of America*, 120(6):3750–3758, 2006.
8. A. Sanada. Extension of the frequency range of normal-incidence sound-absorption-coefficient measurement using four or eight microphones. *Acoustical Science and Technology*, 38(5):261–263, 2017.
9. M. G. Jones. An over-the-rotor liner investigation with configurations enabled by additive manufacturing. NASA/TM-20205010863, 2020.
10. T. L. Parrott and M. G. Jones. Parallel-element liner impedances for improved absorption of broadband sound in ducts. *Noise Control Engineering Journal*, 43(6):183–195, 1995.

**REPORT DOCUMENTATION PAGE**

*Form Approved  
OMB No. 0704-0188*

The public reporting burden for this collection of information is estimated to average 1 hour per response, including the time for reviewing instructions, searching existing data sources, gathering and maintaining the data needed, and completing and reviewing the collection of information. Send comments regarding this burden estimate or any other aspect of this collection of information, including suggestions for reducing this burden, to Department of Defense, Washington Headquarters Services, Directorate for Information Operations and Reports (0704-0188), 1215 Jefferson Davis Highway, Suite 1204, Arlington, VA 22202-4302. Respondents should be aware that notwithstanding any other provision of law, no person shall be subject to any penalty for failing to comply with a collection of information if it does not display a currently valid OMB control number.  
**PLEASE DO NOT RETURN YOUR FORM TO THE ABOVE ADDRESS.**

<b>1. REPORT DATE (DD-MM-YYYY)</b> 01-02-2023		<b>2. REPORT TYPE</b> Technical Memorandum		<b>3. DATES COVERED (From - To)</b>	
<b>4. TITLE AND SUBTITLE</b> High Intensity Modal Impedance Tube Development at NASA Langley				<b>5a. CONTRACT NUMBER</b>	
				<b>5b. GRANT NUMBER</b>	
				<b>5c. PROGRAM ELEMENT NUMBER</b>	
<b>6. AUTHOR(S)</b> Chelsea Solano, Michael G. Jones, Alexander N. Carr, Douglas M. Nark				<b>5d. PROJECT NUMBER</b>	
				<b>5e. TASK NUMBER</b>	
				<b>5f. WORK UNIT NUMBER</b>	
<b>7. PERFORMING ORGANIZATION NAME(S) AND ADDRESS(ES)</b> NASA Langley Research Center Hampton, Virginia 23681-2199				<b>8. PERFORMING ORGANIZATION REPORT NUMBER</b> L-	
<b>9. SPONSORING/MONITORING AGENCY NAME(S) AND ADDRESS(ES)</b> National Aeronautics and Space Administration Washington, DC 20546-0001				<b>10. SPONSOR/MONITOR'S ACRONYM(S)</b> NASA	
				<b>11. SPONSOR/MONITOR'S REPORT NUMBER(S)</b> NASA/TM-20230000292	
<b>12. DISTRIBUTION/AVAILABILITY STATEMENT</b> Unclassified-Unlimited Subject Category Availability: NASA STI Program (757) 864-9658					
<b>13. SUPPLEMENTARY NOTES</b> An electronic version can be found at <a href="http://ntrs.nasa.gov">http://ntrs.nasa.gov</a> .					
<b>14. ABSTRACT</b> A High Intensity Modal Impedance Tube (HIMIT) was developed for evaluation of acoustic liners in a normal incidence, high sound pressure level (SPL), and high frequency environment. Capabilities of the HIMIT are demonstrated here by testing three classes of acoustic liners: a narrow chamber liner, conventional single degree of freedom liners, and over-the-rotor liners. The experimental results are compared to results in NASA Langley's Normal Incidence Tube (NIT) for validation. The Zwikker and Kosten Transmission Line (ZKTL) model is also compared to the HIMIT results for selected configurations to study applicability of the model at high SPLs and frequencies. The HIMIT and NIT impedance spectra compare favorably up to 3.0 kHz, which is the upper frequency limit of the NIT analysis. The ZKTL model was used at frequencies up to 6.0 kHz and showed good agreement with HIMIT results for the entire frequency range tested, indicating that the model may be used at high frequencies when the plane wave mode is dominant.					
<b>15. SUBJECT TERMS</b>					
<b>16. SECURITY CLASSIFICATION OF:</b>			<b>17. LIMITATION OF ABSTRACT</b>	<b>18. NUMBER OF PAGES</b>	<b>19a. NAME OF RESPONSIBLE PERSON</b>
<b>a. REPORT</b>	<b>b. ABSTRACT</b>	<b>c. THIS PAGE</b>			STI Information Desk ( <a href="mailto:help@sti.nasa.gov">help@sti.nasa.gov</a> )
U	U	U	UU		<b>19b. TELEPHONE NUMBER (Include area code)</b> (757) 864-9658